Applied Mathematics & Information Sciences
An International Journal

http://dx.doi.org/10.18576/amis/210105

Bessel Function of the First Kind: Half-Line Addition Theorem

Héctor M. Moya-Cessa

Instituto Nacional de Astrofísica Óptica y Electrónica Calle Luis Enrique Erro No. 1, Santa María Tonantzintla, Pue., 72840, Mexico

Received: 5 Jul. 2026, Revised: 2 Nov. 2026, Accepted: 19 Nov. 2026
Published online: 1 Jan. 2027

Abstract: We study the exponential of the antisymmetric shift generator $\frac{1}{2}(V^\dagger - V)$ on the semi-infinite lattice $\ell^2(\mathbb{N})$, where V is the lowering (Susskind–Glogower) operator. By the method of images we show that its matrix elements are the boundary-corrected Bessel kernel $K_{km}(x) = J_{k-m}(x) + (-1)^m J_{k+m+2}(x)$. The group law and the orthogonality of the displacement operator give, respectively, an addition theorem and orthogonality relations for K_{km}; these are the half-line analogues of the infinite-lattice Bessel identities, of which the classical addition theorem is the prototype. The vacuum column of the kernel, $K_{k0}(x) = 2(k+1)J_{k+1}(x)/x$, yields a Chebyshev–Bessel expansion of $e^{ix\cos t}$ and the sum rule $\sum_{\nu\geq 1} \nu^2 J_\nu(x)^2 = x^2/4$. Acting on the edge site, displacement operators generate normalized, Bessel-weighted coherent-state-like vectors with amplitudes proportional to $(k+1)J_{k+1}(|\alpha|)/|\alpha|$. Because $[V, V^\dagger] = |0\rangle\langle 0| \neq 0$, the three natural ways of composing two displacements with different phases yield different states. The kernel is also the single-particle propagator of a semi-infinite array of evanescently coupled waveguides, in which the image term describes reflection of the diffraction pattern at the array edge.

Keywords: Polynomials; generalized Bessel functions; special functions; nonlinear coherent states.

1 Introduction

Bessel functions of the first kind, $J_k(z)$, are among the most widely used special functions of mathematical physics. They arise whenever a problem has circular or cylindrical symmetry, and they appear in diffraction theory, signal processing and the quantum mechanics of periodic systems [1,2,3]. They also govern light propagation in discrete optics: in an infinite array of identical, evanescently coupled waveguides with nearest-neighbour coupling, the field amplitudes obey a discrete Schrödinger-type equation whose solutions are Bessel functions of integer order [4,5,6]. This observation underlies a fruitful analogy between classical light in engineered photonic lattices and quantum systems: under suitable conditions the dynamics of coupled quantum oscillators can be emulated by purely classical means [7,8,9,10].

Many Bessel identities are manifestations of translation invariance. The classical addition theorem [1, Chap. 11], [3, §10.23], $J_{k-m}(x+y) = \sum_{n\in\mathbb{Z}} J_{k-n}(x)J_{n-m}(y)$, for instance, states that $\exp[\frac{x}{2}(S - S^{-1})]$, with S the bilateral shift on $\ell^2(\mathbb{Z})$, forms a one-parameter group; its matrix elements are $J_{k-m}(x)$, which is why this operator is the propagator of the infinite waveguide array.

Physical lattices, however, are finite and some times they may be considered semi-infinite. A boundary breaks translation invariance: the unilateral shifts $V, V^\dagger$ no longer commute, $[V, V^\dagger] = |0\rangle\langle 0|$, and they generate the Susskind–Glogower algebra rather than the Weyl–Heisenberg algebra [11,12,13]. The semi-infinite array is accordingly harder to treat; it has been approached with phase-operator techniques [11,12] and, in discrete optics, with the method of images [6]. It is therefore natural to ask what replaces the Bessel addition theorem, and what replaces Glauber's coherent states [14], on the half-line.

Two lines of work are closely related. Generalized Bessel functions, which arise when light hops to several neighbours, were developed extensively by Dattoli and co-workers [15,16,17] and have recently been applied to multi-site waveguide couplers [18]. In quantum optics, nonlinear coherent states [19], in particular states built with the Susskind–Glogower operators whose expansion coefficients are Bessel functions, have attracted attention [20,21,22,23].

* Corresponding author e-mail: hmmc@inaoep.mx

© 2027 NSP
Natural Sciences Publishing Cor.

In this paper we answer both questions for the simplest displacement operator on $\ell^2(\mathbb{N})$. Our main results are:

(i) The matrix elements of $\exp[\frac{x}{2}(V^\dagger - V)]$ are

$$K_{km}(x) = J_{k-m}(x) + (-1)^m J_{k+m+2}(x), \qquad k,m \in \mathbb{N}, \tag{1}$$

a Bessel kernel with an "image" correction due to the boundary (Proposition 1). It may also be written as

$$K_{km}(x) = i^{-(k-m)}\,\frac{2}{\pi}\int_0^\pi \sin[(k+1)t] \times \sin[(m+1)t]\, e^{ix\cos t}\, dt. \tag{2}$$

(ii) K obeys the addition theorem $\sum_{n\geq 0} K_{kn}(x)K_{nm}(y) = K_{km}(x+y)$ and the orthogonality relations $\sum_{k\geq 0} K_{km}(x)K_{kn}(x) = \delta_{mn}$ (Theorem 1, Corollary 1). Their vacuum-column specializations give the sum rule $\sum_{\nu\geq 1} \nu^2 J_\nu(x)^2 = x^2/4$ and a Chebyshev–Bessel expansion of $e^{ix\cos t}$.

(iii) Two composite displacements of the edge site with different phases can be applied in either order ("types A and B"); both yield normalized states whose amplitudes are convolution-type Bessel sums. A single displacement by the vector sum ("type C") yields normalized states with amplitudes $\propto (k+1)J_{k+1}(|\alpha|)/|\alpha|$. The three families agree for collinear amplitudes but not otherwise, as a consequence of $[V, V^\dagger] \neq 0$ (Proposition 2).

The paper is organized as follows. Section 2 derives the kernel. Section 3 proves the addition theorem and orthogonality relations and lists the Bessel identities they contain. Section 4 constructs the coherent-state-like families (composite types A and B, then the single-displacement type C) and analyzes their mutual relations. Section 5 contains a discussion and an outlook.

2 The boundary-corrected Bessel kernel

Let $\{|n\rangle\}_{n\geq 0}$ be the orthonormal basis of $\ell^2(\mathbb{N})$ and define

$$V|n\rangle = |n-1\rangle \ \ (n\geq 1), \quad V|0\rangle = 0, \qquad \hat{n}|n\rangle = n|n\rangle. \tag{3}$$

Then $VV^\dagger = 1$, $V^\dagger V = 1 - |0\rangle\langle 0|$ and $[V, V^\dagger] = |0\rangle\langle 0|$.

Set $A = V^\dagger - V$ and define the displacement operator

$$U(x) = e^{\frac{x}{2}A} = e^{\frac{x}{2}(V^\dagger - V)}, \qquad x \in \mathbb{R}. \tag{4}$$

$U(x)$ is a unitary operator, $U(x)^{-1} = U(-x) = U(x)^T$.

Phase rotations. Let $R_\phi = e^{i\phi\hat{n}}$, so that $R_\phi|k\rangle = e^{ik\phi}|k\rangle$. Since $R_\phi V^\dagger R_{-\phi} = e^{i\phi}V^\dagger$ and $R_\phi V R_{-\phi} = e^{-i\phi}V$,

$$R_\phi\, U(x)\, R_{-\phi} = \exp\Big[\tfrac{x}{2}\big(e^{i\phi}V^\dagger - e^{-i\phi}V\big)\Big], \tag{5}$$

and

$$\langle k|\, R_\phi U(x) R_{-\phi}\, |m\rangle = e^{i(k-m)\phi}\, \langle k|\, U(x)\, |m\rangle. \tag{6}$$

Proposition 1(Matrix elements). *For $k,m \in \mathbb{N}$,*

$$\langle k|\, U(x)\, |m\rangle = K_{km}(x) = J_{k-m}(x) + (-1)^m J_{k+m+2}(x).$$

Proof. Let $S|n\rangle = |n+1\rangle$ be the bilateral shift on $\ell^2(\mathbb{Z})$ and $A_\infty = S - S^{-1}$. From the generating function $e^{\frac{x}{2}(z-1/z)} = \sum_{n\in\mathbb{Z}} J_n(x) z^n$, which converges in operator norm for $z = S$ because $|J_n(x)| \leq (|x|/2)^{|n|}/|n|!$, one finds

$$U_\infty(x) = e^{\frac{x}{2}A_\infty} = \sum_{n\in\mathbb{Z}} J_n(x) S^n, \tag{7}$$

and

$$\langle k|\, U_\infty(x)\, |m\rangle = J_{k-m}(x), \quad k,m \in \mathbb{Z}. \tag{8}$$

Define the bounded map $W : \ell^2(\mathbb{N}) \to \ell^2(\mathbb{Z})$ by

$$W|m\rangle = |m\rangle + (-1)^m |-m-2\rangle, \qquad m \geq 0,$$

i.e. an alternating-sign reflection about the "virtual site" -1. We claim $A_\infty W = WA$ on $\ell^2(\mathbb{N})$. For $m \geq 1$, using $A|m\rangle = |m+1\rangle - |m-1\rangle$,

$$\begin{aligned} A_\infty W|m\rangle &= |m+1\rangle - |m-1\rangle + (-1)^m\big(|-m-1\rangle - |-m-3\rangle\big), \\ WA|m\rangle &= W|m+1\rangle - W|m-1\rangle \\ &= |m+1\rangle - |m-1\rangle + (-1)^m\big(|-m-1\rangle - |-m-3\rangle\big), \end{aligned}$$

which agree. For $m = 0$ one has $A|0\rangle = |1\rangle$, so $WA|0\rangle = |1\rangle - |-3\rangle$, while $A_\infty W|0\rangle = A_\infty(|0\rangle + |-2\rangle) = |1\rangle - |-1\rangle + |-1\rangle - |-3\rangle = |1\rangle - |-3\rangle$; the two again agree. Hence $A_\infty W = WA$, and therefore $U_\infty(x)W = WU(x)$. For $k,m \geq 0$ we have

$$\langle k|\, W\, |m\rangle = \delta_{km} + (-1)^m \delta_{k,-m-2} = \delta_{km},$$

because $-m-2 < 0 \leq k$; thus $\langle k|W = \langle k|$ as functionals on $\ell^2(\mathbb{N})$. Consequently, for $k,m \geq 0$,

$$\begin{aligned} \langle k|\, U(x)\, |m\rangle &= \langle k|\, WU(x)\, |m\rangle = \langle k|\, U_\infty(x) W\, |m\rangle \\ &= J_{k-m}(x) + (-1)^m J_{k+m+2}(x). \end{aligned} \tag{9}$$

Remark. [Photonic interpretation] By (6) with $\phi = \pi/2$, $R_{\pi/2}\, U(x)\, R_{-\pi/2} = \exp[\frac{ix}{2}(V + V^\dagger)]$, so that $\langle k|\exp[\frac{ix}{2}(V+V^\dagger)]\,|m\rangle = i^{k-m}K_{km}(x)$. The right-hand side is the single-particle propagator $\exp(-iHz)$ of a semi-infinite array of identical evanescently coupled waveguides, with $H = -c(V + V^\dagger)$ and $x = 2cz$ (the sign of c can be removed by the gauge transformation $(-1)^{\hat{n}}$). The image term $(-1)^m J_{k+m+2}$ describes reflection of the discrete diffraction pattern at the array edge.

Remark. [Spectral representation] The kernel can also be obtained without images. The map $|k\rangle \mapsto \psi_k(t) = \sqrt{2/\pi}\sin[(k+1)t]$ is unitary from $\ell^2(\mathbb{N})$ onto $L^2(0,\pi)$, and $2\cos t\, \psi_k = \psi_{k+1} + \psi_{k-1}$ with $\psi_{-1} \equiv 0$, so $V + V^\dagger$ acts as multiplication by $2\cos t$. Hence

$$\langle k|\exp[\tfrac{ix}{2}(V+V^\dagger)]\,|m\rangle = \frac{2}{\pi}\int_0^\pi \sin[(k+1)t] \times \sin[(m+1)t]\, e^{ix\cos t}\, dt. \tag{10}$$

© 2027 NSP
Natural Sciences Publishing Cor.

Writing the product of sines as $\frac{1}{2}\{\cos[(k-m)t]-\cos[(k+m+2)t]\}$ and using

$$\int_0^\pi \cos\nu t\, e^{ix\cos t}dt = \pi i^\nu J_\nu(x) \tag{11}$$

gives $i^{k-m}\big[J_{k-m}(x)+(-1)^m J_{k+m+2}(x)\big]$, in agreement with Remark 2. In this picture the image term is the Dirichlet condition $\psi=0$ at the virtual site -1. Since $\sin[(k+1)t]=\sin t\,U_k(\cos t)$ with U_k the Chebyshev polynomials of the second kind, the case $m=0$ (see (14) below) is equivalent to the expansion

$$e^{ix\cos t}=\frac{2}{x}\sum_{k=0}^{\infty} i^k\,(k+1)\,J_{k+1}(x)\,U_k(\cos t),$$

which we also confirmed numerically.

Remark. [Edge versus bulk] Since $|J_\nu(x)|\le(|x|/2)^\nu/\nu!$ for $\nu\ge 0$, the image term in (1) is bounded by $(|x|/2)^{k+m+2}/(k+m+2)!$. The image term is already negligible once $k+m+2$ exceeds $|x|$ by a few multiples of $|x|^{1/3}$, where $J_\nu(x)$ enters its exponentially small regime. Far from the boundary, K_{km} therefore reduces to the infinite-lattice kernel J_{k-m}.

3 Addition theorem and orthogonality relations

Theorem 1. *[Addition theorem for the boundary Bessel kernel] For all $x,y\in\mathbb{R}$ and $k,m\in\mathbb{N}$,*

$$\begin{aligned}\sum_{n=0}^{\infty}&\Big[J_{k-n}(x)+(-1)^n J_{k+n+2}(x)\Big]\\&\Big[J_{n-m}(y)+(-1)^m J_{n+m+2}(y)\Big]\\&=J_{k-m}(x+y)+(-1)^m J_{k+m+2}(x+y).\end{aligned}\tag{12}$$

The series converges absolutely.

Proof. Since $\frac{x}{2}A$ and $\frac{y}{2}A$ commute, $U(x)U(y)=U(x+y)$. Taking the matrix element between $\langle k|$ and $|m\rangle$ and inserting $1=\sum_{n\ge0}|n\rangle\langle n|$ between the two factors gives $\sum_n K_{kn}(x)K_{nm}(y)=K_{km}(x+y)$ by Proposition 1. Absolute convergence follows from the superexponential decay of $J_\nu(x)$ and $J_\nu(y)$ as $\nu\to\infty$.

Equation (12) differs from the classical addition theorem for integer-order Bessel functions [1, Chap. 11], [3, §10.23] in two respects: the sum runs over $n\ge0$ instead of $n\in\mathbb{Z}$, and each factor carries an image term. Both modifications originate from the boundary.

Corollary 1. *[Reflection, index swap and orthogonality]*

(a) $K_{km}(-x)=(-1)^{k+m}K_{km}(x)$, *and* $K_{mk}(x)=(-1)^{k+m}K_{km}(x)$.

(b) $\sum_{k=0}^{\infty}K_{km}(x)K_{kn}(x)=\delta_{mn}$ *and* $\sum_{n=0}^{\infty}K_{kn}(x)K_{mn}(x)=\delta_{km}$.

Proof. (a) The reflection identity follows from $J_\nu(-x)=(-1)^\nu J_\nu(x)$. The index-swap relation follows from $J_{m-k}(x)=J_{-(k-m)}(x)=(-1)^{k-m}J_{k-m}(x)$ and $J_{m+k+2}(x)=J_{k+m+2}(x)$:

$$\begin{aligned}K_{mk}(x)&=J_{m-k}(x)+(-1)^k J_{m+k+2}(x)\\&=(-1)^{k-m}J_{k-m}(x)+(-1)^k J_{k+m+2}(x)\\&=(-1)^{k+m}K_{km}(x).\end{aligned}\tag{13}$$

The two displayed forms are thus related by a sign $(-1)^{k+m}$, so K_{km} is symmetric only up to this sign.

(b) Since $U(x)$ is real, $U(x)^T=U(x)^{-1}$. The relation $U(x)^TU(x)=1$ has matrix elements $\delta_{mn}=\sum_{k\ge0}U_{km}(x)U_{kn}(x)=\sum_k K_{km}(x)K_{kn}(x)$, which is the first identity. Likewise $U(x)U(x)^T=1$ gives $\delta_{km}=\sum_{n\ge0}U_{kn}(x)U_{mn}(x)=\sum_n K_{kn}(x)K_{mn}(x)$.

Equivalently, $U(x)$ is orthogonal, i.e. the columns $\{K_{km}(x)\}_{k\ge0}$ form an orthonormal set for each x.

Identities for the *vacuum* column. Using $J_{\nu-1}+J_{\nu+1}=2\nu J_\nu/x$, the column $m=0$ simplifies to

$$K_{k0}(x)=J_k(x)+J_{k+2}(x)=\frac{2(k+1)}{x}J_{k+1}(x).\tag{14}$$

Corollary 1(b) with $m=n=0$ then reads $\sum_{\nu\ge1}\nu^2J_\nu(x)^2=x^2/4$ (the first even moment of the squared Bessel functions, cf. [22]), and (12) with $m=0$ gives

$$\begin{aligned}\sum_{n=0}^{\infty}&\Big[J_{k-n}(x)+(-1)^nJ_{k+n+2}(x)\Big]\frac{(n+1)J_{n+1}(y)}{y}\\&=\frac{(k+1)J_{k+1}(x+y)}{x+y}.\end{aligned}\tag{15}$$

Equation (15) will be used in Section 4, where it expresses that two collinear displacements of the edge site compose.

4 Coherent-state-like vectors on the semi-infinite lattice

Unlike Glauber coherent states, that are generated from the vacuum by the Weyl–Heisenberg displacement operator, the states below are generated by displacement operators built from V and $V^\dagger$ and carry explicit information about the boundary. Throughout, $|0\rangle$ is the edge site. We write $F_{XY}=|\langle\alpha_X|\,\alpha_Y\rangle|^2$ for the pairwise fidelities between the families $X,Y\in\{A,B,C\}$.

4.1 Phase-rotated displacements

For $\alpha=|\alpha|e^{i\phi}\in\mathbb{C}$ define

$$D(\alpha)=\exp\Big(\tfrac{\alpha}{2}V^\dagger-\tfrac{\alpha^*}{2}V\Big)=R_\phi\,U(|\alpha|)\,R_{-\phi},\tag{16}$$

© 2027 NSP
Natural Sciences Publishing Cor.

where the second equality follows from (6). $D(\alpha)$ is unitary, and $D(\alpha)|0\rangle$ is the basic "displaced edge site" of this section. The states below differ in how displacements with different phases are composed, which is controlled by the commutator of their generators.

Proposition 2(Non-commuting generators). *Let* $X_\alpha = \frac{1}{2}(\alpha V^\dagger - \alpha^* V)$. *Then*

$$[X_\alpha, X_\beta] = \tfrac{i}{2}\,\mathrm{Im}(\alpha\beta^*)\,|0\rangle\langle 0|\,.$$

Hence X_α *and* X_β *commute if and only if* α *and* β *are collinear (i.e.* $\mathrm{Im}(\alpha\beta^*) = 0$*).*

*Proof.*Using $[V^\dagger, V] = -|0\rangle\langle 0|$ and $[V, V^\dagger] = |0\rangle\langle 0|$, $[X_\alpha, X_\beta] = \frac{1}{4}\big(-\alpha\beta^*[V^\dagger, V] - \alpha^*\beta[V, V^\dagger]\big) = \frac{1}{4}(\alpha\beta^* - \alpha^*\beta)\,|0\rangle\langle 0|$, and $\alpha\beta^* - \alpha^*\beta = 2i\,\mathrm{Im}(\alpha\beta^*)$.

For collinear α, β the generators commute and $D(\alpha)D(\beta) = D(\alpha+\beta)$ (this is (12) in disguise). Otherwise the ways of composing two displacements with different phases need not agree. We first define the two composite families A and B, and then the single-displacement family C.

4.2 Composite displacements: types A and B

Fix $x, y > 0$ and a relative phase $\theta \in \mathbb{R}$; by (16), $D(xe^{i\theta}) = R_\theta U(x) R_{-\theta}$ and $D(y) = U(y)$. By (6) and Proposition 1,

$$\langle k|\,D(xe^{i\theta})\,|m\rangle = K_{km}(x)\,e^{i(k-m)\theta},\ \langle k|\,D(y)\,|m\rangle = K_{km}(y).$$

Since the two generators do not commute, applying them to the edge site in the two possible orders gives two different states.

Type A. Displace first by y and then by $xe^{i\theta}$:

$$|\alpha_A\rangle = D(xe^{i\theta})\,D(y)\,|0\rangle = R_\theta\,U(x)\,R_{-\theta}\,U(y)\,|0\rangle\,. \quad (17)$$

Inserting $1 = \sum_{m\geq 0}|m\rangle\langle m|$ between the two factors and using (17) together with the vacuum column (14), $\langle m|\,U(y)\,|0\rangle = K_{m0}(y) = J_m(y) + J_{m+2}(y)$, we obtain

$$|\alpha_A\rangle = \sum_{k=0}^{\infty}\sum_{m=0}^{\infty}\Big[J_{k-m}(x) + (-1)^m J_{k+m+2}(x)\Big] \Big[J_m(y) + J_{m+2}(y)\Big]\,e^{i(k-m)\theta}\,|k\rangle\,. \quad (18)$$

Type B. Displace first by $xe^{i\theta}$ and then by y:

$$|\alpha_B\rangle = D(y)\,D(xe^{i\theta})\,|0\rangle = U(y)\,R_\theta\,U(x)\,R_{-\theta}\,|0\rangle\,. \quad (19)$$

Because $R_{-\theta}\,|0\rangle = |0\rangle$, the same procedure gives

$$|\alpha_B\rangle = \sum_{k=0}^{\infty}\sum_{m=0}^{\infty}\Big[J_{k-m}(y) + (-1)^m J_{k+m+2}(y)\Big] \Big[J_m(x) + J_{m+2}(x)\Big]\,e^{im\theta}\,|k\rangle\,. \quad (20)$$

Both states are unitary images of $|0\rangle$ and are therefore normalized, and both reduce to $|0\rangle$ when $x = y = 0$. Their amplitudes (18) and (20) are sums of convolution-type at the intermediate site m, and the probabilities of site-occupation depend on θ and on both x and y.

Edge amplitudes. The edge component of each state is a single series in the vacuum column of the kernel. From Corollary 1(a), $K_{0m}(x) = (-1)^m K_{m0}(x)$, and hence, with (14),

$$\langle 0|\,\alpha_A\rangle = \sum_{m=0}^{\infty}(-1)^m K_{m0}(x)K_{m0}(y)\,e^{-im\theta} = \frac{4}{xy}\sum_{m=0}^{\infty}(m+1)^2 J_{m+1}(x)J_{m+1}(y)\,e^{-im(\theta+\pi)}, \quad (21)$$

and

$$\langle 0|\,\alpha_B\rangle = \sum_{m=0}^{\infty}(-1)^m K_{m0}(x)K_{m0}(y)\,e^{+im\theta} = \frac{4}{xy}\sum_{m=0}^{\infty}(m+1)^2 J_{m+1}(x)J_{m+1}(y)\,e^{+im(\theta+\pi)}. \quad (22)$$

Since the Bessel functions are real, $\langle 0|\,\alpha_B\rangle = \langle 0|\,\alpha_A\rangle^*$; the two edge probabilities $|\langle 0|\,\alpha_{A,B}\rangle|^2$ therefore coincide even though the states differ elsewhere on the lattice.

4.3 Single displacement: type C

Displacing the edge site by the vector sum $\alpha = y + xe^{i\theta} = |\alpha|e^{i\phi}$ with the single operator (16) gives

$$|\alpha_C\rangle = D(\alpha)\,|0\rangle = \sum_{k=0}^{\infty}\big[J_k(|\alpha|) + J_{k+2}(|\alpha|)\big]e^{ik\phi}\,|k\rangle = \frac{2}{|\alpha|}\sum_{k=0}^{\infty}(k+1)J_{k+1}(|\alpha|)\,e^{ik\phi}\,|k\rangle\,, \quad (23)$$

the type-C state; the amplitudes follow from Proposition 1 and (14). Explicitly, $|\alpha| = \sqrt{(y + x\cos\theta)^2 + x^2\sin^2\theta}$ and $\phi = \arg\alpha$ (computed with the two-argument arctangent, so that ϕ is correct also when $y + x\cos\theta < 0$). It is normalized, depends continuously on α, reduces to $|0\rangle$ for $\alpha \to 0$, and has edge-site overlap $\langle 0|\,\alpha_C\rangle = 2J_1(|\alpha|)/|\alpha|$, which is real. Its site-occupation probabilities $|\langle k|\,\alpha_C\rangle|^2$ depend only on $|\alpha|$. For real α its amplitudes are the Bessel-weighted coefficients of the Susskind–Glogower nonlinear coherent states studied in [20,22].

4.4 Comparison of the three families

Proposition 3(Collinear limit). *For* $\theta \in \{0, \pi\}$ *the three families coincide,* $|\alpha_A\rangle = |\alpha_B\rangle = |\alpha_C\rangle = U(y \pm x)\,|0\rangle$ *(upper sign for* $\theta = 0$*), and the series (22)–(23) sum to* $2J_1(y \pm x)/(y \pm x)$.

© 2027 NSP
Natural Sciences Publishing Cor.

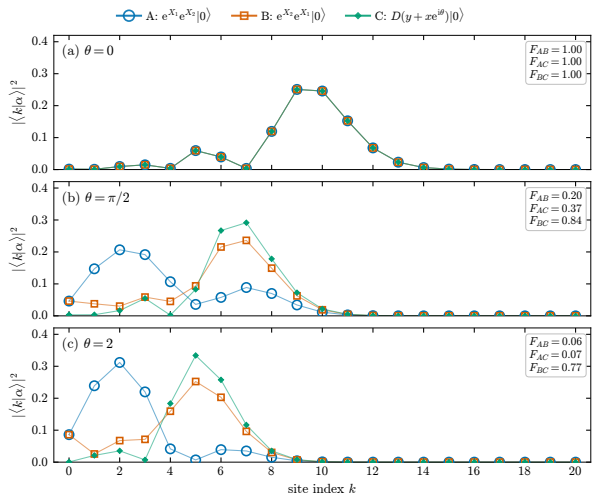


Fig. 1: Site-occupation probabilities $|\langle k|\alpha\rangle|^2$ of the types A (open circles), B (open squares) and C (filled diamonds) for $x = 8$, $y = 4$ and (a) $\theta = 0$, (b) $\theta = \pi/2$, (c) $\theta = 2$. Type C is evaluated at $\alpha = y + x\,e^{i\theta}$. Markers are nested in size so that coincident points remain visible; thin lines are guides to the eye. For $\theta = 0$ the three families coincide. For generic θ they differ in lobe position and in the structure near the edge $k = 0$. The boxes list the pairwise fidelities $F_{XY} = |\langle\alpha_X|\alpha_Y\rangle|^2$.

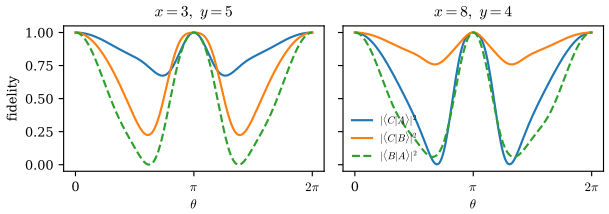


Fig. 2: Pairwise fidelities $F_{XY} = |\langle\alpha_X|\alpha_Y\rangle|^2$ between the families as functions of θ for (a) $(x,y) = (3,5)$ and (b) $(x,y) = (8,4)$. All curves equal unity at $\theta = 0,\pi$ (collinear amplitudes) and fall off between them.

Proof. For $\theta = 0$ and $\theta = \pi$ the amplitudes $xe^{i\theta} = \pm x$ and y are collinear, so by Proposition 2 the generators commute, $R_\pi U(x) R_{-\pi} = U(-x)$, and the group law gives $D(xe^{i\theta})D(y) = D(y)D(xe^{i\theta}) = D(y + xe^{i\theta}) = U(y \pm x)$ (for a negative argument, $D(\alpha) = U(\alpha)$ because $R_\pi U(|\alpha|)R_{-\pi} = U(-|\alpha|)$). The edge amplitude is then $K_{00}(y \pm x) = 2J_1(y \pm x)/(y \pm x)$. In particular, for $\theta = 0$ the series (22) equals $\sum_m K_{0m}(x)K_{m0}(y) = K_{00}(x + y)$, which is (15) with $k = 0$.

Relation between the three families. Types A and B are the products $D(xe^{i\theta})D(y)$ and $D(y)D(xe^{i\theta})$ acting on the edge state, whereas type C is the single displacement $D(y + xe^{i\theta})$. The fidelities of the three states measure the failure of $D(\alpha)D(\beta) = D(\alpha + \beta)$ for non-collinear amplitudes, and are quantified in Figs. 1 and 2. As a numerical example, for $x = 8$, $y = 4$, $\theta = 2$ a direct evaluation of the three states in a truncated lattice gives $F_{AB} \approx 0.063$, $F_{AC} \approx 0.068$ and $F_{BC} \approx 0.77$. We also verified numerically that (18), (20), (23), (22) and (23) agree with the operator definitions to machine precision.

5 Discussion and outlook

The boundary-corrected kernel (1) is the propagator of the displacement operator on the half-line, and its algebraic properties—addition theorem, reflection/index-swap relations, and orthogonality—are inherited directly from the group law and unitarity of $U(x)$. The extra terms $(-1)^m J_{k+m+2}$ are the image contributions of the boundary and become negligible far from it. The Bessel identities derived here are therefore consequences of a single operator statement, and each has a transparent meaning in a semi-infinite waveguide array (Remark 2).

The states $|\alpha_C\rangle = D(\alpha)|0\rangle$ are normalized, continuous in α and reduce to the edge site at $\alpha = 0$, but they are not orbits of a representation of a Lie group: $D(\alpha)D(\beta) \neq D(\alpha + \beta)$ in general, with equality guaranteed only for collinear α and β. They are therefore generalized coherent states in the broad sense of displaced reference states [24,25], and not in the group-theoretical sense of Perelomov [26]. This also explains why the composite families A, B and C of Section 4 differ (Proposition 2).

The occupation-number moments of $|\alpha_C\rangle$ reduce to sums of the form $\sum_\nu \nu^n J_\nu(|\alpha|)^2$, whose closed forms are studied in [22,23]; such moments determine, for instance, the Mandel Q parameter [27] of the corresponding intensity distribution. Further directions are semi-infinite arrays with several-neighbour couplings [18], where the image construction must be combined with the generalized Bessel functions of [15,16,17], and time-dependent couplings.

References

[1] Watson, G.N. *A Treatise on the Theory of Bessel Functions*, 2nd ed.; Cambridge University Press: Cambridge, UK, 1944. (No DOI.)

[2] Gradshteyn, I.S.; Ryzhik, I.M. *Table of Integrals, Series, and Products*, 8th ed.; Zwillinger, D., Moll, V., Eds.; Academic Press: Amsterdam, The Netherlands, 2014; ISBN 978-0-12-384933-5.

[3] Olver, F.W.J.; Olde Daalhuis, A.B.; Lozier, D.W.; Schneider, B.I.; Boisvert, R.F.; Clark, C.W.; Miller, B.R.; Saunders, B.V. (Eds.) *NIST Digital Library of Mathematical Functions*. Available online: https://dlmf.nist.gov/ (accessed

© 2027 NSP
Natural Sciences Publishing Cor.

on 15 September 2023); see Chapter 10, §10.23 for addition theorems.
[4] Jones, A.L. Coupling of optical fibers and scattering in fibers. *J. Opt. Soc. Am.* **1965**, *55*, 261–269. https://doi.org/10.1364/JOSA.55.000261
[5] Christodoulides, D.N.; Lederer, F.; Silberberg, Y. Discretizing light behaviour in linear and nonlinear waveguide lattices. *Nature* **2003**, *424*, 817–823. https://doi.org/10.1038/nature01936
[6] Makris, K.G.; Christodoulides, D.N. Method of images in optical discrete systems. *Phys. Rev. E* **2006**, *73*, 036616. https://doi.org/10.1103/PhysRevE.73.036616
[7] Longhi, S. Quantum-optical analogies using photonic structures. *Laser Photonics Rev.* **2009**, *3*, 243–261. https://doi.org/10.1002/lpor.200810055
[8] Fernández Guasti, M.; Moya-Cessa, H. Amplitude and phase representation of quantum invariants for the time-dependent harmonic oscillator. *Phys. Rev. A* **2003**, *67*, 063803. https://doi.org/10.1103/PhysRevA.67.063803
[9] Urzúa, A.R.; Ramos-Prieto, I.; Fernández-Guasti, M.; Moya-Cessa, H.M. Solution to the time dependent coupled harmonic oscillators Hamiltonian with arbitrary interactions. *Quantum Rep.* **2019**, *1*, 82–90. https://doi.org/10.3390/quantum1010008
[10] Moya-Cessa, H.M.; Soto-Eguibar, F. *Introduction to Quantum Optics*; Rinton Press: Paramus, NJ, USA, 2011; ISBN 978-1-58949-061-1.
[11] London, F. Über die Jacobischen Transformationen der Quantenmechanik. *Z. Phys.* **1926**, *37*, 915–925. https://doi.org/10.1007/BF01397491
[12] Susskind, L.; Glogower, J. Quantum mechanical phase and time operator. *Physics Physique Fizika* **1964**, *1*, 49–61. https://doi.org/10.1103/PhysicsPhysiqueFizika.1.49
[13] Carruthers, P.; Nieto, M.M. Phase and angle variables in quantum mechanics. *Rev. Mod. Phys.* **1968**, *40*, 411–440. https://doi.org/10.1103/RevModPhys.40.411
[14] Glauber, R.J. Coherent and incoherent states of the radiation field. *Phys. Rev.* **1963**, *131*, 2766–2788. https://doi.org/10.1103/PhysRev.131.2766
[15] Dattoli, G.; Giannessi, L.; Richetta, M.; Torre, A. Miscellaneous results on infinite series of Bessel functions. *Nuovo Cimento B* **1989**, *103*, 149–159. https://doi.org/10.1007/BF02891769
[16] Dattoli, G.; Giannessi, L.; Mezi, L.; Torre, A. Theory of generalized Bessel functions. *Nuovo Cimento B* **1990**, *105*, 327–348. https://doi.org/10.1007/BF02726105
[17] Dattoli, G.; Torre, A.; Lorenzutta, S.; Maino, G.; Chiccoli, C. Theory of generalized Bessel functions—II. *Nuovo Cimento B* **1991**, *106*, 21–51. https://doi.org/10.1007/BF02723125
[18] Tapia-Valerdi, M.A.; Ramos-Prieto, I.; Soto-Eguibar, F.; Moya-Cessa, H.M. Waveguide arrays: Interaction to many neighbors. *Dynamics* **2025**, *5*, 25. https://doi.org/10.3390/dynamics5030025
[19] Man'ko, V.I.; Marmo, G.; Sudarshan, E.C.G.; Zaccaria, F. f-Oscillators and nonlinear coherent states. *Phys. Scr.* **1997**, *55*, 528–541. https://doi.org/10.1088/0031-8949/55/5/004
[20] León-Montiel, R. de J.; Moya-Cessa, H.M.; Soto-Eguibar, F. Nonlinear coherent states for the Susskind–Glogower operators. *Rev. Mex. Fís. S* **2011**, *57*(3), 133–147. http://rmf.smf.mx/pdf/rmf-s/57/3/57_3_133.pdf (no DOI found).
[21] Gazeau, J.-P.; Hussin, V.; Moran, J.; Zelaya, K. Generalized Susskind–Glogower coherent states. *J. Math. Phys.* **2021**, *62*, 072104. https://doi.org/10.1063/5.0043743
[22] Moya-Cessa, H.M. Bessel moment polynomials. *Appl. Math. Inf. Sci.* **2026**, *20*, 1371–1375. https://doi.org/10.18576/amis/200519
[23] Moya-Cessa, H.M. Closed forms for odd moments of squared Bessel functions. *Appl. Math. Inf. Sci.* **2027**, *21*, 19–30. https://doi.org/10.18576/amis/210102
[24] Klauder, J.R. Continuous-representation theory. I. Postulates of continuous-representation theory. *J. Math. Phys.* **1963**, *4*, 1055–1058. https://doi.org/10.1063/1.1704034
[25] Gazeau, J.-P. *Coherent States in Quantum Physics*; Wiley-VCH: Weinheim, Germany, 2009; ISBN 978-3-527-40709-5.
[26] Perelomov, A.M. Coherent states for arbitrary Lie group. *Commun. Math. Phys.* **1972**, *26*, 222–236. https://doi.org/10.1007/BF01645091
[27] Mandel, L. Sub-Poissonian photon statistics in resonance fluorescence. *Opt. Lett.* **1979**, *4*, 205–207. https://doi.org/10.1364/OL.4.000205

Héctor M. Moya-Cessa obtained his PhD at Imperial College in 1993 and since then he is a researcher/lecturer at Instituto Nacional de Astrofísica, Óptica y Electrónica in Puebla, Mexico where he works on Quantum Optics. He has published over 220 papers in international peer reviewed journals. He is fellow of the Alexander von Humboldt Foundation.

© 2027 NSP
Natural Sciences Publishing Cor.